

## Cell Ashing for Trace Element Analysis: A New Approach Based on Ultraviolet/Ozone

Gelsomina De Stasio,<sup>\*†·1</sup> B. Gilbert,<sup>\* L. Perfetti,‡ R. Hansen,§ D. Mercanti,<sup>¶</sup> M. T. Ciotti,<sup>¶</sup> R. Andres,<sup>|| V. E. White,\*\* P. Perfetti,† and G. Margaritondo<sup>\*††</sup></sup></sup>

<sup>\*</sup>*Institut de Physique Appliquée, Ecole Polytechnique Fédérale, PH-Ecublens, CH-1015 Lausanne, Switzerland; †Istituto di Struttura della Materia del CNR, Via Fosso del Cavaliere, Rome, Italy; ‡Università di Roma "Tor Vergata," Rome, Italy; §Synchrotron Radiation Center, University of Wisconsin, Stoughton, Wisconsin 53589; ¶Istituto di Neurobiologia del Consiglio Nazionale delle Ricerche, Viale Marx 15, 00137 Rome, Italy; ||Paul Scherrer Institut, CH 5232 Villigen PSI, Switzerland; \*\*Jet Propulsion Laboratory, California Institute of Technology, 4800 Oak Grove Drive, Pasadena, California 91109-8099; and ††Sincrotrone Trieste SCpA, Trieste, Italy*

Received March 11, 1998

**We studied a new approach to cell ashing based on illuminating the specimens with a low-pressure mercury discharge lamp. We analyzed with synchrotron spectromicroscopy its effects on different physiological elements in neurobiological specimens. Our results demonstrate that carbon is removed, whereas phosphorus, calcium, potassium, and sulfur are retained and their relative concentrations are enhanced. Applied to trace elements, this technique will enhance their practical detectability.** © 1999 Academic Press

**Key Words:** synchrotron spectromicroscopy; microchemical analysis; MEPHISTO; ashing; incineration; trace element.

Ashing is often used to reduce the thickness of tissue sections or to investigate the chemical properties of biological specimens (1–4). This procedure should eliminate certain elements (carbon, nitrogen, and hydrogen) and enhance the relative concentration of others, thus improving their detectability. Its effects on the specimen structure (2) and chemistry (1) have been extensively analyzed.

Conventional ashing is based on high-temperature incineration or on the exposure to oxygen plasma (1–4). We adopted a different technique, based on the illumination of the specimens with a UV lamp at atmospheric pressure and room temperature. This ap-

proach has distinct advantages over conventional techniques because the use of photons (massless and with zero kinetic energy, and consequently no ballistic effects) ensures that the remaining elements are not displaced while carbon is removed. This is particularly important for spatially resolved chemical analysis. More conventional approaches alter the element spatial distribution by high-energy oxygen bombardment, high temperature, or sputtering.

We present synchrotron spectromicroscopy (5–7) results on the chemical effects of UV/ozone ashing of neurobiological specimens compared to unashed specimens, demonstrating that this procedure does not introduce detectable element redistribution. The data include spectromicroscopy images, spectra, and elemental distribution maps.

### MATERIALS AND METHODS

Synchrotron spectromicroscopy analyzes the chemical composition and the state of elements on a microscopic scale (5–7). The technique consists of illuminating the specimen with monochromatized X rays emitted by a synchrotron light source (here, the 10-m toroidal-grating monochromator beamline of the Wisconsin Synchrotron Radiation Center storage ring Aladdin) and detecting the emitted photoelectrons. The photoelectron intensity vs photon energy curves mirror the absorption coefficient; from characteristic spectroscopic features one derives the presence and chemical state of the corresponding element (8).

We analyzed ashed and unashed neurobiological specimens with the MEPHISTO spectromicroscope (5) with a submicrometer spatial resolution. The speci-

<sup>1</sup>To whom correspondence should be addressed at Istituto di Struttura della Materia, Consiglio Nazionale delle Ricerche, Via Fosso del Cavaliere, I-00133 Rome, Italy. Fax: +39-6-4993-4153. E-mail: pupa@src.wisc.edu.



**FIG. 1.** Micrograph of an ashed granule cell culture on a gold-coated stainless-steel substrate. The image was acquired with 174-eV photons. Note the characteristic appearance of cell bodies and neuronal processes preserved after ashing.

mens were primary cultures of rat cerebellar granule cells. A detailed description of the specimen preparation process can be found in Refs. (6) and (7). In short, cells extracted from rat cerebellum were allowed to grow for 8 days on gold-coated stainless-steel substrates, pretreated with 10  $\mu\text{g/ml}$  of poly-L-lysine solution. Selective techniques were used to obtain a prevailing population of granule cells (9–11).

At the end of the growth period, the cultures were washed, fixed with 4% paraformaldehyde in PBS<sup>2</sup> for 20 min, then carefully washed twice to remove the excess fixative and the PBS salts, and finally air-dried. Note that any chemical modification of the cells induced by paraformaldehyde or PBS is common to all samples, ashed and nonashed, and cannot therefore introduce any artifacts in the results obtained, which are meant to be only comparative. Part of the cultures were analyzed in this form, and others were first ashed by exposing them to the UV light and ozone produced by a low-pressure mercury-discharge lamp in a desiccator cabinet. Filtered air was pumped through the cabinet at a rate of about 2 liters per minute to supply oxygen and remove reaction products. The effluent gas was passed through a column of activated charcoal to neutralize the ozone.

Ashing occurs under UV illumination because ozone produced by photodissociation of oxygen reacts with organic carbon to produce volatile products (CO and CO<sub>2</sub>) (12–16). This type of lamp has been recently used to remove the radiation-induced carbon contamination from synchrotron optical elements exposed to X rays (12–14).

<sup>2</sup> Abbreviation used: PBS, phosphate-buffered saline.

A low-pressure mercury lamp emits two photon wavelengths relevant to carbon removal: 1850 and 2537 Å. The 1850-Å light generates ozone in air by photodissociation of oxygen, and the 2537-Å light photosensitizes organic carbon enhancing the carbon-removal rate. The 2537-Å light also causes photodecomposition of ozone.

The ozone-degrading 2537-Å light travels farther in air than the ozone-producing 1850-Å light—thus producing a strong ozone concentration gradient around the lamp. Therefore, the carbon removal rates strongly depend on the lamp distance (12). In the present study, the lamp specimens' distance was 5 mm. The exposure time varied between 6 and 48 h, with complete carbon removal only after 48 h.

## RESULTS AND DISCUSSION

All images and spectra reported below are representative of a much larger database that we acquired over a period of 10 months, on different types of cells in culture, including rat cerebellar neurons, glial cells, meningioma cells, fibroblasts, and human brain tissue sections from glioblastoma and meningioma patients. All these samples originated from at least 20 separate biological/bioptical preparations, and yielded very similar results after ashing for all the physiological elements reported below.

Figure 1 shows a MEPHISTO micrograph of a portion of a neuron culture ashed for 48 h. The contrast is caused by the different photoelectron emission yield of different elements. The image was acquired at 174 eV photon energy, for which sulfur photoemits more than gold: therefore, the S-containing cells appear brighter than the gold substrate.

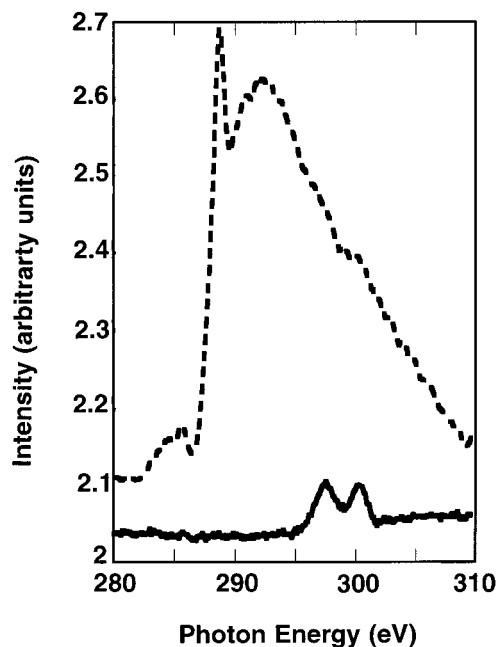


**FIG. 2.** X-ray absorption curves in the C1s and K2p edge spectral region taken on ashed (solid line) and unashed (dashed line) neuron cells. Carbon is removed and the K2p edge becomes prominent after ashing. The ashed spectrum was taken on a  $25 \times 15 \mu\text{m}^2$  area on the cell cluster in the lower-central part of Fig. 1. The unashed curve was taken on the same sample before ashing. Both spectra were normalized to the monochromator output and smoothed.

The dark,  $\approx 5\text{-}\mu\text{m}$ -size round-shaped features are cell bodies. They appear dark due to their three-dimensional shape: MEPHISTO has a low collection efficiency for electrons emitted by surfaces not perpendicular to its optical axis.

The elongated bright features are the axons and dendrites, characteristic of the neuron networks. Note that they maintain their typical morphology after ashing, at least in two dimensions.

MEPHISTO can acquire X-ray absorption spectra from selected microscopic areas by measuring the electron yield while scanning the photon energy. These spectra reveal the microchemical composition of specific features such as cell structures (5).

Figures 2–7 show results obtained in the spectral regions of the C1s, K2p, N1s, O1s, Ca2p, P2p, and S2p edges. All spectra reported in Figs. 2–7 from ashed cells were acquired from a  $25 \times 15 \mu\text{m}^2$  area in the cell cluster in the lower-central part of Fig. 1. The unashed cell spectra were taken from the same sample before it was ashed. The spectra were normalized to the monochromator yield curve. These spectra do not represent a quantitative analysis, which is never possible with spectromicroscopy (5). Nevertheless, the detection limit of the instrument was measured to be 100 ppm. The only safe quantitative statement we can make about the spectra in Figs. 2–7 is, therefore, that the detected

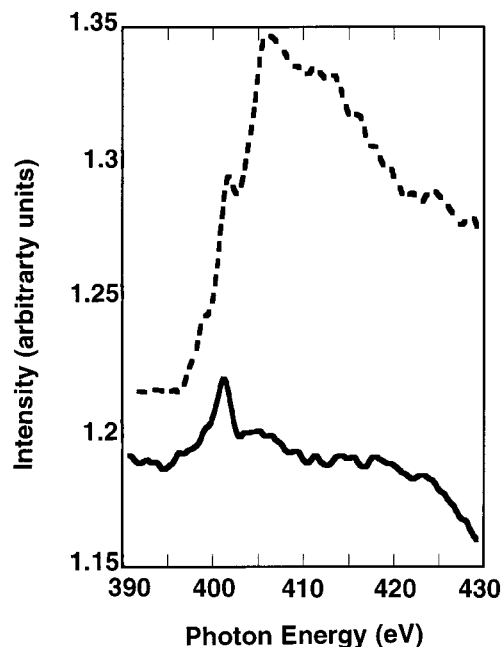


**FIG. 3.** N1s edge spectra: nitrogen is not completely removed by ashing but the lineshape changes.

elements must have had a surface concentration higher than 100 ppm.

In all spectra the solid and dashed curves correspond to ashed and unashed specimens.

Figure 2 shows that carbon is completely removed by ashing. Note that this UV/ozone technique was developed to completely remove carbon from semiconductors

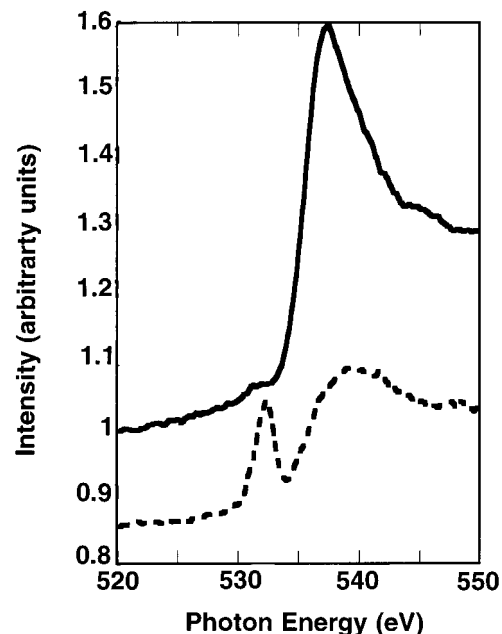


**FIG. 4.** O1s edge spectra before and after ashing.

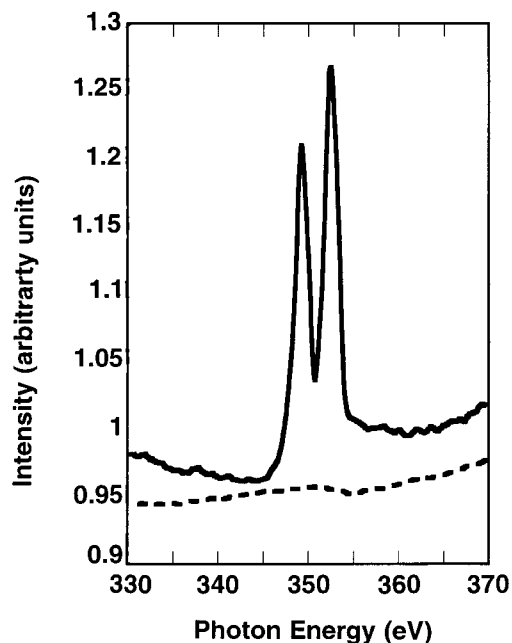


FIG. 5. Ca2p edge spectra: the previously undetectable calcium signal is very intense after ashing.

and optical elements, and it has been proven to be extremely effective (12–17). The central goal of the present experiment was to demonstrate that with the same method carbon can be effectively removed from cells, as Fig. 2 proves.

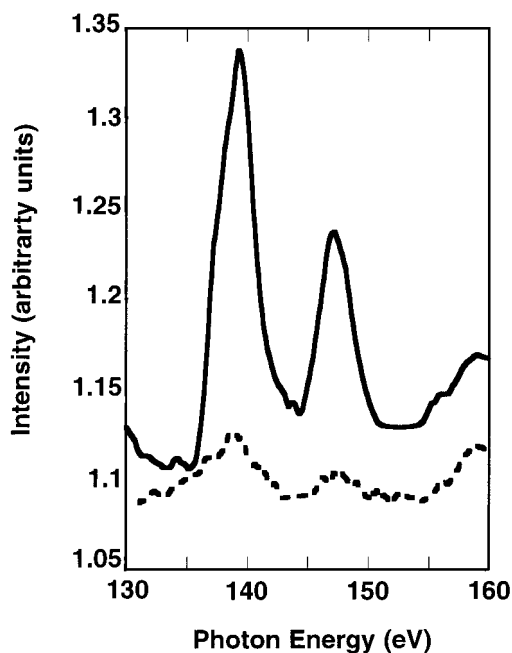


FIG. 6. P2p edge spectra. The unashed specimen curve was corrected to remove second-order C peaks at 142 and 145 eV.

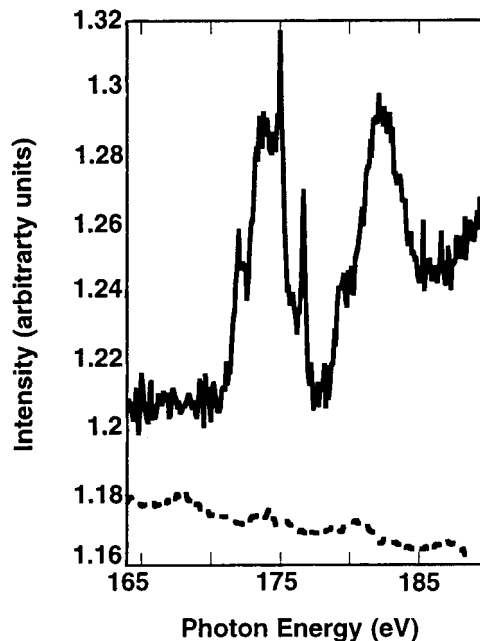


FIG. 7. Ashing enhancement of the S2p edge. To avoid losing the sharp features at 172, 175, 176.7, and 179.5 eV, the ashed specimen curve was left unsmoothed.

We analyzed the samples after 6, 12, 24, 36, and 48 h of UV/ozone exposure, and saw C1s completely removed only after 48 h. We have therefore adopted this criterion to judge the ashing time required.

In Fig. 2 we observe that potassium is practically not detectable before ashing, even if its peaks are visible in the unashed spectrum because it overlaps the C1's spectral features, and is therefore almost impossible to deconvolve from this latter without a perfectly accurate knowledge of C1's structures without potassium, which is never available in a biological specimen. In the ashed spectrum of Fig. 2 potassium becomes more prominent with its characteristic spectral features above 295 eV.

Figure 3 indicates the presence of nitrogen even after ashing; however, the 401-eV peak is very intense in both spectra, whereas the broad spectral features at higher energies are weakened by ashing. The permanence of a strong 401 eV peak—due to the  $-\text{NH}_2$  aminic group in basic amino acids and/or to the  $-\text{CONHC}$  group in peptide bonds (17)—is consistent with previous data (1) on oxygen-plasma ashing. Note that this peak is still present even after 65 h of UV/ozone ashing (data not shown). The weakening of the other features has not yet been clarified.

Figure 4 shows that oxygen, as expected, is not removed by ashing; but its chemical state is dramatically altered. The unashed spectrum has the "typical" line-shape of oxygen in the gas phase or in organic compounds (17). The intense spectral feature in the ashed spectrum must be a combination of ashing-induced

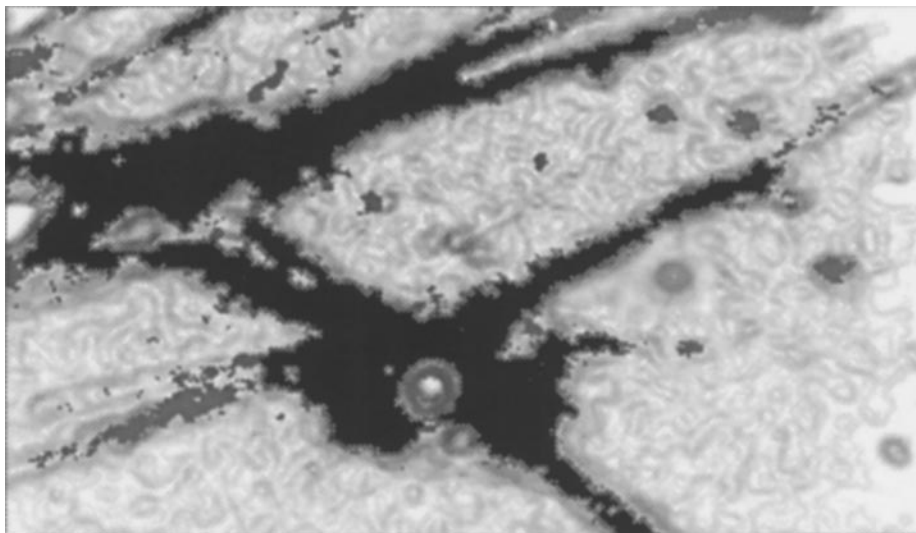


**FIG. 8.** Calcium distribution map, obtained by dividing pixel by pixel an image acquired at 349 eV (Ca2p peak) by an off-peak image at 340 eV. The Ca map (black) is superimposed on an intensity-reduced edge-enhanced version of Fig. 1.

oxides of several other elements. We speculate these may be, for example,  $-\text{PO}_4$ ,  $-\text{SO}_4$ ,  $\text{Cl}_2\text{O}$ ,  $\text{Na}_2\text{O}$ ,  $\text{NaOH}$ ,  $\text{K}_2\text{O}$ ,  $\text{KOH}$ ,  $\text{CaO}$ ,  $\text{Ca}(\text{OH})_2$ .

The central point of our data is the enhancement of the calcium, phosphorus, potassium, and sulfur concentrations by ashing. Previously undetectable potassium, calcium, and sulfur become very prominent in Figs. 2, 5, and 7. Phosphorus is already visible before ashing but strongly ashing-enhanced—see Fig. 6.

Figures 8–11 show the calcium, phosphorus, sulfur, and potassium spatial distribution maps. Each map is the pixel-by-pixel ratio of two different images: one at the maximum-emission photon energy of the mapped

element and the other at a below-edge energy for which the element does not emit.

Each distribution map is shown superimposed on an edge-enhanced weak-intensity version of Fig. 1. The maps show that P, S, and Ca are localized on the cell structures and virtually absent from the substrate. In the case of K, unfortunately, the low signal level (see Fig. 2) resulted in the noisy map of Fig. 11 with probably spurious potassium signal in substrate areas. This result, given the low signal-to-noise ratio, cannot be interpreted as a reliable distribution map of potassium.

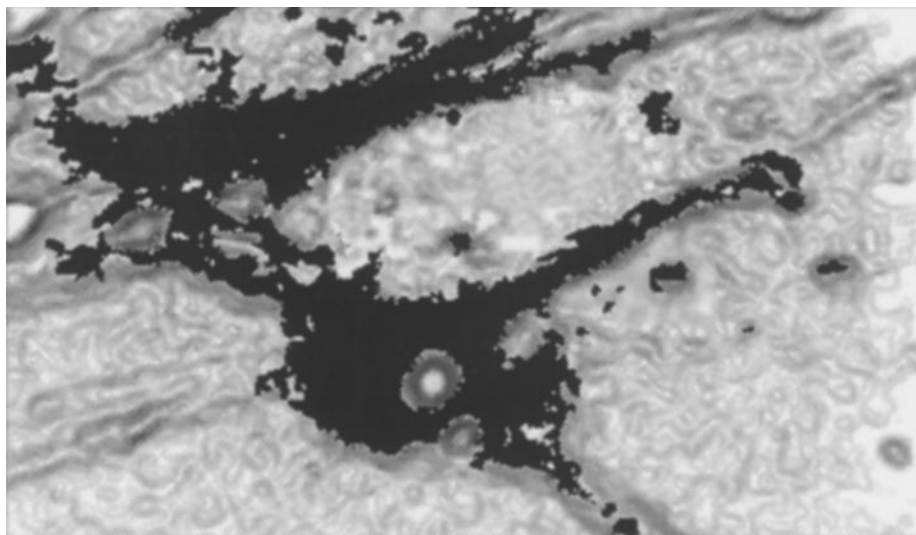


**FIG. 9.** Phosphorus distribution map obtained with the same strategy of Fig. 8, but derived from images at 149 and 133 eV.

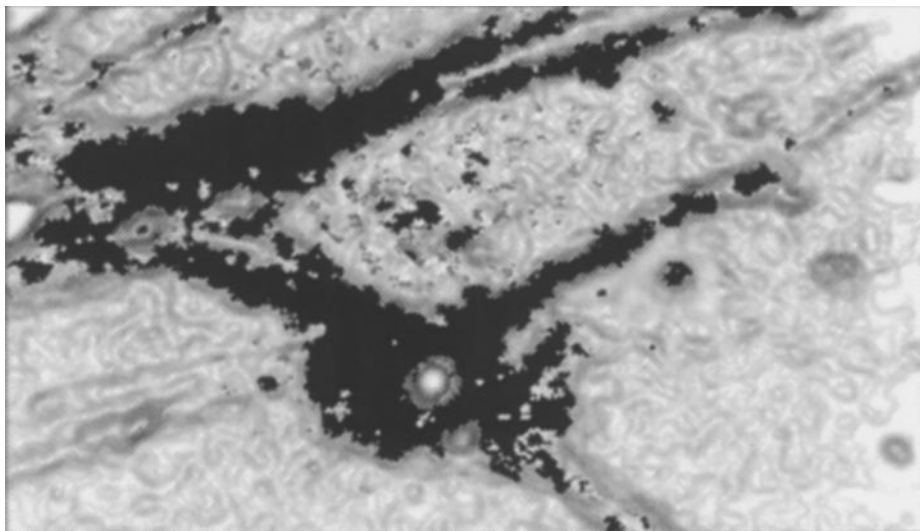


**FIG. 10.** Sulfur distribution map derived from images at 174 and 170 eV.

## CONCLUSIONS

Our first finding is that carbon is eliminated by our new ashing process, as hoped. Note that carbon removal occurs independently of the original chemical state (C-chain, aromatic compounds, macromolecules, lipids, etc.) of carbon in the cells. Second, nitrogen and oxygen are not completely removed, and their chemical state appears to be altered by ashing. Third and most important, the signal intensity of calcium, phosphorous, potassium, and sulfur is dramatically increased. This enabled us, in particular, to obtain reliable distribution maps of most of these previously undetectable elements.

Please note that when we say that carbon is removed by UV/ozone ashing, we mean removed from the sur-

face of the sample. We can in fact detect the presence or absence of elements only in the first 100 Å of the sample surface. There is a possibility that carbon is still present in samples, "buried" under a surface layer of other carbon-free physiological elements. Such a layer might be protecting the inner carbon from oxidation and removal.

Compared to more conventional ashing techniques, such as the oxygen plasma which we extensively studied and characterized (1), the UV/ozone approach appears advantageous. With oxygen plasma C is efficiently removed, N is reduced, and the relative concentration of the other elements is increased, but on the other hand the technique redistributes elements inside and outside the cell structures. We have recently

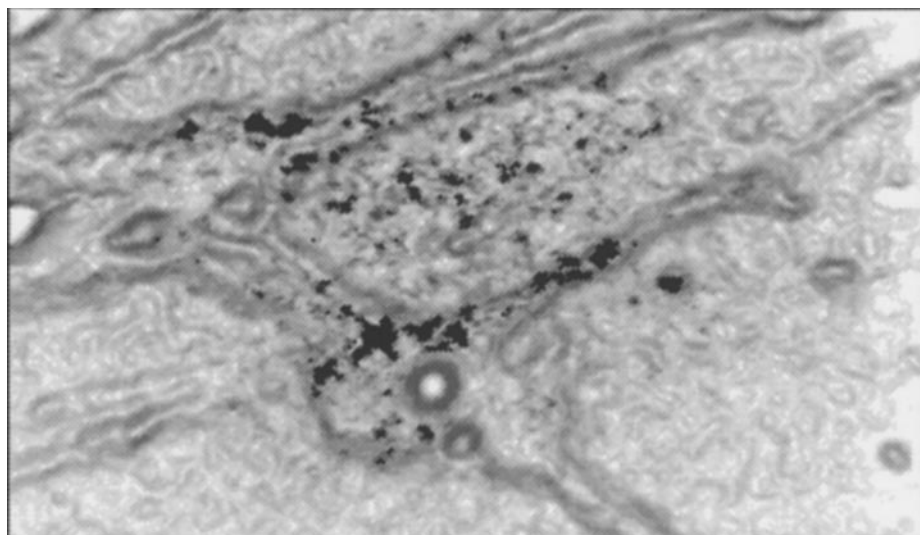


**FIG. 11.** Potassium distribution map derived from images at 297 and 292 eV.

observed this happening systematically and have tentatively interpreted it with a fairly simple model: the oxygen ions bombarding the sample surface have high kinetic energy ( $>1$  keV). They practically sputter the sample, transferring to the constituent elements impulse and kinetic energy, and therefore redistributing them around.

With this interpretation in mind we decided to explore the new ashing strategy with UV/ozone. In this approach, in fact, the ozone and oxygen ions interacting with the sample surface have only thermal energy (0.026 eV), and the UV photons are massless, zero kinetic energy and low photon energy ( $<7$  eV), and cannot effectively displace materials.

The elemental distribution maps of Figs. 8, 9, and 10 demonstrate that sulfur, phosphorus, and calcium are never dislocated outside the cells, on substrate areas. We believe, therefore, that this novel UV/ozone method is superior to oxygen plasma for microchemical studies.

Our new UV/ozone ashing applied to biological specimens can greatly facilitate the study of low-concentration elements. It may, for example, allow the detection of trace elements as required for many physiology and pathology investigations.

#### ACKNOWLEDGMENTS

Work was supported by the Fonds National Suisse de la Recherche Scientifique, by the Consiglio Nazionale delle Ricerche and by the Ecole Polytechnique Fédérale de Lausanne. We are indebted to Tom Nelson, Dan Wallace, Mario Capozzi, and the entire staff of the Wisconsin Synchrotron Radiation Center (a national facility supported by the NSF) for their expert professional help.

#### REFERENCES

1. De Stasio, G., Capozzi, M., Droubay, T. C., Mercanti, D., Ciotti, M. T., Lorusso, G. F., Andres, R., Suda, T., Perfetti, P., Tonner, B. P., and Margaritondo, G. (1997) *Anal. Biochem.* **252**, 106–109.
2. Larsson, B., Schwitzer, P. M., Stepanek, J., Teichmann, S., Weinreich, R., Luetolf, U., Romer, M., and Spycher, M. A. (1994) *Hadrontherapy in Oncology* (Amaldi, U., and Larsson, B., Eds.). Elsevier, Amsterdam, and the references therein.
3. Bellanger, J. R. (1995) *J. AOAC Int.* **78**, 477.
4. Davicco, M.-J., Coxam, V., Gaumet, N., Lebecque, P., and Barlet, J.-P. (1995) *Exp. Physiol.* **80**, 449.
5. De Stasio, G., Capozzi, M., Lorusso, G. F., Baudat, P. A., Croubay, T. C., Perfetti, P., Margaritondo, G., and Tonner, B. P. (1998) *Rev. Sci. Instrum.* **69**, 2062–2067.
6. De Stasio, G., Hardcastle, S., Koranda, S. F., Tonner, B. P., Mercanti, D., Ciotti, M. T., Perfetti, P., and Margaritondo, G. (1993) *Phys. Rev.* **E47**, 2117.
7. De Stasio, G., Dunham, D., Tonner, B. P., *et al.* (1993) *Neuro-Report* **4**, 1175, and the references therein.
8. Gudat, W., and Kunz, C. (1972) *Phys. Rev. Lett.* **29**, 169.
9. Aloisi, F., Ciotti, M. T., and Levi, G. (1985) *J. Neurosci.* **5**, 2001.
10. Stichel, C. C., and Müller, H. W. (1991) *Dev. Brain Res.* **64**, 145.
11. Wilkin, G. P., Levi, G., Johnstone, S., *et al.* (1983) *Dev. Brain Res.* **10**, 265–267.
12. Hansen, R. W. C., Bissen, M., Wallace, D., and Miller, T. (1993) *Appl. Optics* **32**, 4114–4116.
13. Hansen, R. W. C., Wolske, J., and Takacs, P. Z. (1994) *Nucl. Instrum. Methods* **A347**, 254–257.
14. Hansen, R. W. C., Wolske, J., Wallace, D., and Bissen, M. (1994) *Nucl. Instrum. Methods* **A347**, 249–253.
15. Vig, J. R. (1985) *J. Vac. Sci. Technol.* **A3**, 1027–1034.
16. Kern, W. (Ed.) (1993) *Handbook of Semiconductor Cleaning Technology*, pp. 233–273. Noyes, Park Ridge, NJ.
17. Muilenberg, G. E. (Ed.) (1979) *Handbook of X-Ray Photoelectron Spectroscopy*. Perkin-Elmer, Eden Prairie MN.